

1 **Idiosyncratic, retinotopic bias in face identification**
2 **modulated by familiarity**

3 Abbreviated title: Retinotopic bias in face identification

4 Matteo Visconti di Oleggio Castello^{1,*}, Morgan Taylor¹, Patrick Cavanagh^{1,2},
5 M. Ida Gobbini^{1,3,*}

6 ¹Department of Psychological & Brain Sciences,
7 Dartmouth College,
8 Hanover NH, 03755, USA

9 ²Department of Psychology
10 Glendon College
11 Toronto ON, M4N 3M6 Canada

12 ³Dipartimento di Medicina Specialistica, Diagnostica, e Sperimentale,
13 University of Bologna,
14 40100 Bologna, Italy

15 * corresponding authors:

16 M. Ida Gobbini, mariaida.gobbini@unibo.it
17 Matteo Visconti di Oleggio Castello, mvddoc.gr@dartmouth.edu
18 6207 Moore Hall
19 Dartmouth College
20 Hanover, NH 03755, USA

21

22 Number of pages: 47

23 Number of figures: 5

24 Number of tables: 3

25 Words (Abstract): 155

26 Words (Introduction): 831

27 Words (Discussion): 2,133

28

29 **Conflict of Interest**

30 The authors declare no competing financial interests.

31

32 **Acknowledgments**

33 We would like to thank the Martens Family Fund and Dartmouth College for their
34 support. We would like to thank Carlo Cipolli for helpful discussion.

35 **Abstract**

36 The perception of gender and age of unfamiliar faces is reported to vary
37 idiosyncratically across retinal locations such that, for example, the same
38 androgynous face may appear to be male at one location but female at another. Here
39 we test spatial heterogeneity for the recognition of the *identity* of personally familiar
40 faces in human participants. We found idiosyncratic biases that were stable within
41 participants and that varied more across locations for low as compared to high
42 familiar faces. These data suggest that like face gender and age, face identity is
43 processed, in part, by independent populations of neurons monitoring restricted
44 spatial regions and that the recognition responses vary for the same face across these
45 different locations. Moreover, repeated and varied social interactions appear to lead
46 to adjustments of these independent face recognition neurons so that the same
47 familiar face is eventually more likely to elicit the same recognition response across
48 widely separated visual field locations.

49 **Significance statement**

50 In this work we tested spatial heterogeneity for the recognition of personally familiar
51 faces. We found retinotopic biases that varied more across locations for low as
52 compared to highly familiar faces. The retinotopic biases were idiosyncratic and
53 stable within participants. Our data suggest that, like face gender and age, face
54 identity is processed by independent populations of neurons monitoring restricted

55 spatial regions and that recognition may vary for the same face at these different
56 locations. Unlike previous findings, our data show how the effect of learning modifies
57 the representation of face identity in cortical areas with spatially restricted receptive
58 fields. This new perspective has broader implications for understanding how learning
59 optimizes visual processes for socially salient stimuli.

60 **Introduction**

61 We spend most of our days interacting with acquaintances, family and close friends.
62 Because of these repeated and protracted interactions, the representation of
63 personally familiar faces is rich and complex, as reflected by stronger and more
64 widespread neural activation in the distributed face processing network, as compared
65 to responses to unfamiliar faces (Gobbini and Haxby, 2007; Taylor et al., 2009;
66 Gobbini, 2010; Natu and O'Toole, 2011; Bobes et al., 2013; Sugiura, 2014; Ramon and
67 Gobbini, 2017; Visconti di Oleggio Castello et al., 2017a). Differences in
68 representations are also reflected in faster detection and more robust recognition of
69 familiar faces (Burton et al., 1999; Gobbini et al., 2013; Ramon et al., 2015; Visconti di
70 Oleggio Castello and Gobbini, 2015; Visconti di Oleggio Castello et al., 2017b). Thus,
71 despite the subjective feeling of expertise with faces in general (Diamond and Carey,
72 1986), our visual system seems to be optimized for the processing of familiar faces.
73 The mechanisms underlying the prioritized processing of familiar faces are still a
74 matter of investigation (Guntupalli and Gobbini, 2017; Ramon and Gobbini, 2017;
75 Young and Burton, 2017).

76 The advantage for familiar faces could originate at different stages of the face
77 processing system. The classic psychological model by Bruce and Young (1986) posits
78 that recognition of familiar faces occurs when the structural encoding of a perceived
79 face matches stored representations (Bruce and Young, 1986). In this model the
80 stored representations of familiar faces consist of “an interlinked set of expression-
81 independent structural codes for distinct head angles, with some codes reflecting the
82 global configuration at each angle and others representing particular distinctive
83 features” (Bruce and Young, 1986, p. 309). Behavioral evidence supports the
84 hypothesis that local features are processed differentially for personally familiar faces.
85 For example, in a study of perception of gaze direction and head angle, changes in eye
86 gaze were detected around 100ms faster in familiar than in unfamiliar faces (Visconti
87 di Oleggio Castello and Gobbin, 2015). In another study, the advantage for personally
88 familiar faces was maintained after face inversion, a manipulation that is generally
89 thought to reduce holistic processing in favor of local processing (Visconti di Oleggio
90 Castello et al., 2017b).

91 Could local features be sufficient to initially drive a differential response to personally
92 familiar faces? In a study measuring saccadic reaction time, correct and reliable
93 saccades to familiar faces were recorded as fast as 180 ms when unfamiliar faces were
94 distractors (Visconti di Oleggio Castello and Gobbin, 2015). In an EEG study using
95 multivariate analyses, significant decoding of familiarity could be detected at around
96 140 ms from stimulus onset (Barragan-Jason et al., 2015). At such short latencies it is
97 unlikely that a viewpoint-invariant representation of an individual face’s identity

98 drives these differential responses. To account for facilitated, rapid detection of
99 familiarity, we have previously hypothesized that personally familiar faces may be
100 recognized quickly based on diagnostic, idiosyncratic features, which become highly
101 learned through extensive personal interactions (Visconti di Oleggio Castello and
102 Gobbin, 2015; Visconti di Oleggio Castello et al., 2017b). Detection of these features
103 may occur early in the face-processing system, allowing an initial, fast differential
104 processing for personally familiar faces.

105 Processes occurring at early stages of the visual system can show idiosyncratic
106 retinotopic biases (Greenwood et al., 2017). Afray et al. (2010) reported retinotopic
107 biases for perceiving face gender and age that varied depending on stimulus location
108 in the visual field and were specific to each subject. These results suggest that
109 diagnostic facial features for gender and age are encoded in visual areas with limited
110 position invariance. Neuroimaging studies have shown that face-processing areas
111 such as OFA, pFus, and mFus have spatially restricted population receptive fields that
112 could result in retinotopic differences (Kay et al., 2015; Silson et al., 2016; Grill-Spector
113 et al., 2017b). Here we hypothesized that detectors of diagnostic visual features that
114 play a role in identification of familiar faces may also show idiosyncratic retinotopic
115 biases and that these biases may be tuned by repeated interactions with personally
116 familiar faces. Such biases may affect recognition of the identities presented in
117 different parts of the visual field and may be modulated by the familiarity of those
118 identities.

119 We tested this hypothesis by presenting participants with morphed stimuli of
120 personally familiar individuals that were briefly shown at different retinal locations. In
121 two separate experiments we found that participants showed idiosyncratic biases for
122 specific identities in different visual field locations, and these biases were stable on
123 retesting after weeks. Importantly, the range of the retinal biases was inversely
124 correlated with the reported familiarity of each target identity, suggesting that
125 prolonged personal interactions with the target individuals reduced retinal biases.
126 These findings provide additional support for the hypothesis that asymmetries in the
127 processing of personally familiar faces can arise at stages of the face-processing
128 system where there is reduced position invariance and where local features are being
129 processed, such as in OFA or perhaps even earlier. Our results show that prolonged,
130 personal interactions can modify the neural representation of faces at this early level
131 of processing.

132 Materials and Methods

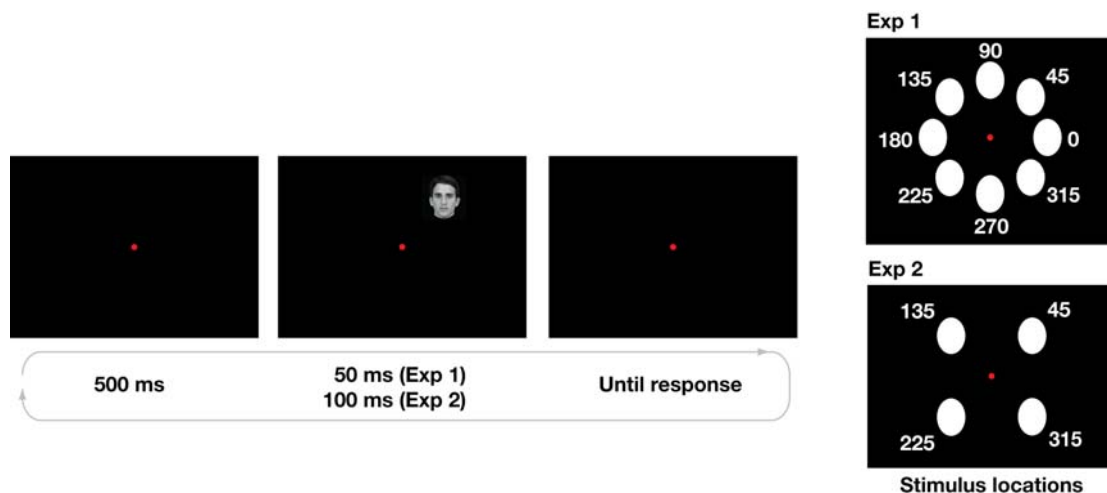


Figure 1. Experimental paradigm. The left panel shows an example of the

experimental paradigm, while the right panel shows the locations used in Experiment 1 (eight locations, top panel) and in Experiment 2 (four locations, bottom panel).

133 ***Stimuli***

134 Pictures of the faces of individuals who were personally familiar to the participants
135 (graduate students in the same department) were taken in a photo studio room with
136 the same lighting condition and the same camera. Images of two individuals were
137 used for Experiment 1, and images of three individuals were used for Experiment 2. All
138 individuals portrayed in the stimuli signed written informed consent for the use of
139 their pictures for research and in publications.

140 The images were converted to grayscale, resized and centered so that the eyes were
141 aligned in the same position for the three identities, and the background was
142 manually removed. These operations were performed using ImageMagick and Adobe
143 Photoshop CS4. The resulting images were matched in luminance (average pixel
144 intensity) using the SHINE toolbox (function *lumMatch*) (Willenbockel et al., 2010)
145 after applying an oval mask, so that only pixels belonging to the face were modified.
146 The luminance-matched images were then used to create morph continua (between
147 two identities in Experiment 1, see Figure 2; and among three identities in Experiment
148 2, see Figure 3) using Abrosoft Fantamorph (v. 5.4.7) with seven percentages of
149 morphing: 0, 17, 33, 50, 67, 83, 100 (see Figures 2, 3).

150 **Experiment 1**

151 *Paradigm*

152 The experimental paradigm was similar to that by Afraz et al., (2010). In every trial
153 participants would see a briefly flashed image in one of eight locations at the
154 periphery of their visual field (see Figure 1). Each image was shown for 50 ms at a
155 distance of 7° of visual angle from the fixation point, and subtended approximately 4°
156 x 4° of visual angle. The images could appear in one of eight locations evenly spaced
157 by 45 angular degrees around fixation. For Experiment 1, only the morph *ab* was used
158 (see Figure 1). Participants were required to maintain fixation on a central red dot
159 subtending approximately 1° of visual angle.

160 After the image disappeared, participants reported which identity they saw using the
161 left (identity *a*) and right (identity *b*) arrow keys. There was no time limit for
162 responding, and participants were asked to be as accurate as possible. After
163 responding, participants had to press the spacebar key to continue to the next trial.

164 Participants performed five blocks containing 112 trials each, for a total of 560 trials.
165 In each block all the images appeared twice for every angular location (8 angular
166 locations x 7 morph percentages x 2 = 112). This provided ten data points for each
167 percentage morphing at each location, for a total of 70 trials at each angular location.

168 Before the experimental session participants were shown the identities used in the
169 experiment (corresponding to 0% and 100% morphing, see Figure 2), and practiced

170 the task with 20 trials. These data were discarded from the analyses. Participants
171 performed two identical experimental sessions at least four weeks apart.

172 Participants sat at a distance of approximately 50 cm from the screen, with their chin
173 positioned on a chin-rest. The experiment was run using Psychtoolbox (Kleiner et al.,
174 2007) (version 3.0.12) in MATLAB (R2014b). The screen operated at a resolution of
175 1920x1200 and a 60Hz refresh rate.

176 *Subjects*

177 We recruited six subjects for this experiment (three males, including one of the
178 authors, MVdOC). The sample size for Experiment 1 was not determined by formal
179 estimates of power, and was limited by the availability of participants familiar with the
180 stimulus identities. After the first experimental session, two participants (one male,
181 one female) were at chance level in the task, thus only data from four subjects (two
182 males, mean age 27.50 ± 2.08 SD) were used for the final analyses.

183 All subjects had normal or corrected-to-normal vision, and provided written informed
184 consent to participate in the experiment. The study was approved by the Dartmouth
185 College Committee for the Protection of Human Subjects.

186 **Experiment 2**

187 *Paradigm*

188 Experiment 2 differed from Experiment 1 in the following parameters (see Figures 1,
189 3): 1. three morph continua (*ab*, *ac*, *bc*) instead of one; 2. images appeared in four
190 locations (45° , 135° , 225° , 315°) instead of eight; 3. images were shown for 100 ms
191 instead of 50 ms to make the task easier.

192 All other parameters were the same as in Experiment 1. Participants had to indicate
193 which of the three identities they saw by pressing the left (identity *a*), right (identity
194 *b*), or down (identity *c*) arrow keys.

195 Participants performed ten blocks containing 84 trials each, for a total of 840 trials. In
196 each block all the images appeared once for every angular location (4 angular
197 locations x 7 morph percentages x 3 morphs = 84). We used 70 data points at every
198 angular location to fit the model for each pair of identities. Thus, we used the
199 responses to different unmorphed images for each pair of identities, ensuring
200 independence of the models.

201 Before the experimental session participants were shown the identities used in the
202 experiment (corresponding to 0% and 100% morphing, see Figure 3), and practiced
203 the task with 20 trials. These data were discarded from the analyses. Participants
204 performed two experimental sessions at least four weeks apart.

205 *Subjects*

206 Ten participants (five males, mean age 27.30 ± 1.34 SD) participated in Experiment 2,
207 five of which were recruited for Experiment 1 as well. No authors participated in
208 Experiment 2. The sample size ($n = 10$) was determined using G*Power3 (Faul et al.,
209 2007, 2009) to obtain 80% power at $\alpha = 0.05$ based on the correlation of the PSE
210 estimates across sessions in Experiment 1, using a bivariate normal model (one-
211 tailed).

212 All subjects had normal or corrected-to-normal vision, and provided written informed
213 consent to participate in the experiment. The study was approved by the Dartmouth
214 College Committee for the Protection of Human Subjects.

215 ***Familiarity and contact scales***

216 After the two experimental sessions, participants completed a questionnaire designed
217 to assess how familiar each participant was with the identities shown in the
218 experiment. Participants saw each target identity, and were asked to complete
219 various scales for that identity. The questionnaire comprised the "Inclusion of the
220 Other in the Self" scale (IOS) (Aron et al., 1992; Gächter et al., 2015), the "Subjective
221 Closeness Inventory" (SCI) (Berscheid et al., 1989), and the "We-scale" (Cialdini et al.,
222 1997). The IOS scale showed two circles increasingly overlapping labeled "You" and
223 "X", and participants were given the following instructions: *Using the figure below*
224 *select which pair of circles best describes your relationship with this person. In the figure*
225 *"X" serves as a placeholder for the person shown in the image at the beginning of this*

226 *section, and you should think of "X" being that person. By selecting the appropriate*
227 *number please indicate to what extent you and this person are connected (Aron et al.,*
228 *1992; Gächter et al., 2015). The SCI scale comprised the two following questions:*
229 *Relative to all your other relationships (both same and opposite sex) how would you*
230 *characterize your relationship with the person shown at the beginning of this section?,*
231 *and Relative to what you know about other people's close relationships, how would you*
232 *characterize your relationship with the person shown at the beginning of this section?*
233 Participants responded with a number between one (*Not close at all*) and seven (*Very*
234 *close*) (Berscheid et al., 1989). The We-scale comprised the following question: *Please*
235 *select the appropriate number below to indicate to what extent you would use the term*
236 *"WE" to characterize you and the person shown at the beginning of this section.*
237 Participants responded with a number between one (*Not at all*) and seven (*Very much*
238 *so*). For each participant and each identity we created a composite "familiarity score"
239 by averaging the scores in the three scales.

240 We also introduced a scale aimed at estimating the amount of interaction or contact
241 between the participant and the target identity. The scale was based on the work by
242 Idson and Mischel (2001), and participants were asked to respond Yes/No to the
243 following six questions: *Have you ever seen him during a departmental event?, Have you*
244 *ever seen him during a party?, Have you ever had a group lunch/dinner/drinks with him?,*
245 *Have you ever had a one-on-one lunch/dinner/drinks with him?, Have you ever texted*
246 *him personally (not a group message)?, and Have you ever emailed him personally (not a*

247 *group email*)? The responses were converted to 0/1 and for each participant and for
248 each identity we created a “contact score” by summing all the responses.

249 For each subject separately, to obtain a measure of familiarity and contact related to
250 each morph, we averaged the familiarity and contact scores of each pair of identities
251 (e.g., the familiarity score of morph *ab* was the average of the scores for identity *a* and
252 identity *b*).

253 ***Psychometric fit***

254 For both experiments we fitted a group-level psychometric curve using Logit Mixed-
255 Effect models (Moscatelli et al., 2012) as implemented in *lme4* (Bates et al., 2015). For
256 each experiment and each session, we fitted a model of the form

$$y^k = \text{logit}\left(\beta_0 x + \sum_{i=1}^n (\beta_i + z_i^k) I_i\right)$$

257 where *k* indicates the subject, *n* is the number of angular locations (*n* = 8 for the first
258 experiment, and *n* = 4 for the second experiment), *I_i* is an indicator variable for the
259 angular location, β_i are the model fixed-effects, and *z_i* are the subject-level random-
260 effects (random intercept). From this model, we defined for each subject the Point of
261 Subjective Equality (PSE) as the point *x* such that $\text{logit}(x) = 0.5$, that is for each angular
262 location

$$PSE_i^k = -\frac{\beta_i}{\beta_0} - \frac{z_i^k}{\beta_0} = PSE_i^p + \Delta PSE_i^k$$

263 Thus, the PSE for subject k at angular location i can be decomposed in a population-
264 level PSE and a subject-specific deviation from the population level, indicated with
265 PSE^p and ΔPSE^k respectively.

266 In Experiment 2 we fitted three separate models for each of the morph continua. In
267 addition, prior to fitting we removed all trials in which subjects mistakenly reported a
268 third identity. For example, if an image belonging to morph ab was presented, and
269 subjects responded with c , the trial was removed.

270 To quantify the bias across locations, we computed a variance score by squaring the
271 $\Delta PSE_{i,j}$, and summing them across locations, that is $bias = \sum_{i=1}^4 (\Delta PSE_i)^2$. Because
272 this quantity is proportional to the variance against 0, throughout the manuscript we
273 refer to it as ΔPSE variance.

274 **Computational modeling**

275 To account for the retinotopic biases we simulated a population of neural units using
276 the Compressive Spatial Summation model (Kay et al., 2013, 2015). This model was
277 originally developed as an encoding model (Naselaris et al., 2011) to predict BOLD
278 responses and estimate population receptive fields in visual areas and face-responsive
279 areas such as OFA, pFus, and mFus (Kay et al., 2015). We refer to activations of neural
280 units that can be thought as being voxels, small populations of neurons, or individual
281 neurons.

282 The CSS model posits that the response of a neural unit is equal to

$$r = g \cdot a^n$$

283 with $a = \int G(x, y | x_0, y_0, \sigma) S(x, y) dx dy$, and $G(x, y | x_0, y_0, \sigma)$ being a 2D gaussian
284 centered at x_0, y_0 , with covariance $\Sigma = \sigma I$, and $S(x, y)$ being the stimulus converted
285 into contrast map. The term g represents the gain of the response, while the power
286 exponent n accounts for subadditive responses (Kay et al., 2013). In our simulations
287 we set $n = 0.2$ as in Kay et al. (2015) when the parameter was not explicitly optimized.
288 Note that the median estimates of n in the three ROIs of interest (IOG, pFus, and
289 mFus) reported by Kay et al. (2015) were 0.20, 0.16, and 0.23 respectively.

290 We simulated a population of $N = N_a + N_b$ neural units, where N_a indicates the number
291 of units selective to identity a , and N_b indicates the number of units selective to
292 identity b . For simplicity we set $N_b = 1$ and varied N_a , effectively changing the ratio of
293 units selective to one of the two identities. The stimuli consisted of contrast circles of
294 diameter 4° centered at 7° from the center, and placed at an angle of $45^\circ, 135^\circ, 225^\circ,$
295 and 315° , simulating Experiment 2. We simulated the activation of the units assuming
296 i.i.d. random noise normally distributed with mean of 0 and standard deviation of 0.1.

297 Each experiment consisted of a learning phase in which we simulated the (noisy)
298 response to the full identities a and b in each of the four locations, with 10 trials for
299 each identity and location. We used these responses to train a Support Vector
300 Machine (Cortes and Vapnik, 1995) with linear kernel to differentiate between the two
301 identities based on the pattern of population responses. Then, we simulated the
302 actual experiment by generating responses to morphed faces. For simplicity, we

303 assumed a linear response between the amount of morphing and the population
304 response. That is, we assumed that if a morph with m percentage morphing towards b
305 was presented, the population response was a combination of the responses to a and
306 b , weighted by $(1-m, m)$. The amounts of morphing paralleled those used in the two
307 experiments (0, 17, 33, 50, 67, 83, 100). We simulated 10 trials for each angular location
308 and each amount of morphing, and recorded the responses of the trained decoder.
309 These responses were used to fit a logit model similar to the model used in the main
310 analyses (without random effects), and to estimate the Point of Subjective Equality
311 for each angular location. The sum of these squared estimates around 50% was
312 computed and stored.

313 We varied systematically the ratio N_a/N_b of units responsive to identity a , ranging from
314 1 to 9, and repeated 500 experiments for each ratio. For each experiment, eccentricity
315 and receptive field size of the units were randomly sampled from a normal bivariate
316 distribution with mean (μ_{ecc}, μ_{size}) and covariance Σ . Once a given sample of
317 eccentricity was drawn, it was converted to a random location lying on the circle of
318 given eccentricity. We also simulated attentional modulations by modifying the gain
319 for the units responsive to identity a between 1 and 4 in 0.5 steps, and fixing the gain
320 for identity b to 1. We simulated receptive fields in this way from three face-
321 responsive ROIs (Inferior Occipital Gyrus, IOG—also termed OFA—mFus, and pFus).

322 We obtained the parameter estimates for (μ_{ecc}, μ_{size}) from published results reported
323 in Kay et al. (2015). In particular, we used the median estimates of eccentricity and

324 receptive field size from Kay et al. (2015) to estimate (μ_{ecc}, μ_{size}) (obtained from
325 Figure S2 for the “face” task). For the three simulated ROIs (IOG, pFus, mFus) these
326 values were $(2.05^\circ, 2.75^\circ)$, $(2.45^\circ, 3.68^\circ)$, and $(1.86^\circ, 3.41^\circ)$ respectively. To estimate Σ ,
327 we assumed a standard deviation of 0.5° for both eccentricity and receptive field size,
328 and we used the regression fit between eccentricity and receptive field size to
329 estimate their covariance (see Figure S2 in Kay et al., 2015). Prior to estimation, the
330 receptive field sizes were scaled back to pixel values by multiplying them by n , with n
331 = 0.2 in all simulations. The covariances thus estimated were 0.0546, 0.0541, and
332 0.0768 for IOG, mFus, and pFus respectively. Data values were extracted from Figure
333 S2 in Kay et al. (2015) using WebPlotDigitizer (<https://automeris.io/WebPlotDigitizer>).

334 ***Code and data availability***

335 Code for the analyses, raw data for both experiments, single subject results, and
336 simulations are available at [REDACTED] as well as Extended Data.

337 **Results**

338 ***Experiment 1***

339 In this experiment, participants performed a two-alternative forced-choice (AFC) task
340 on identity discrimination. In each trial they saw a face presented for 50 ms, and were
341 asked to indicate which of the two identities they just saw. Each face could appear in
342 one of eight stimulus locations. Participants performed the same experiment with the

343 same task a second time, at least 33 days after the first session (average 35 days \pm 4
 344 days standard deviation).

345 Participants showed stable and idiosyncratic retinal heterogeneity for identification.
 346 The PSE estimates for the two sessions were significantly correlated (see Table 1 and
 347 Figure 2B), showing stable estimates, and the within-subject correlations of Δ PSEs
 348 (see Methods) was significantly higher than the between-subject correlation
 349 (correlation difference: 0.87 [0.64, 1.10], 95% BCa confidence intervals (Efron, 1987);
 350 see Table 2), showing that the biases were idiosyncratic (see Figure 2A for example
 351 fits for two different subjects).

Table 1. Correlation of parameter estimates across sessions for the two experiments.				
Parameter	r	t	df	p
Experiment 1				
PSE	0.89 [-0.23, 1]	4.86**	6	0.002831
Δ PSE	0.71 [0.47, 0.84]	5.47***	30	6.106e-06
Experiment 2				
PSE	0.98 [0.93, 0.99]	15.22***	10	3.042e-08
Δ PSE	0.64 [0.5, 0.75]	9.02***	118	3.997e-15
Note: All confidence intervals are 95% BCa with 10,000 repetitions. * $p < .05$. ** $p < .01$. *** $p < .001$				

352

Table 2. Comparison of within-subjects correlations of parameter estimates across sessions with between-subjects correlations.			
Morph	Within-subjects r	Between-subjects r	Difference

Experiment 1			
ab	0.65 [†] [0.57, 0.8]	-0.22 [-0.41, -0.01]	0.87 [†] [0.63, 1.1]
Experiment 2			
ab	0.32 [-0.10, 0.62]	-0.02 [-0.15, 0.11]	0.34 [-0.07, 0.69]
ac	0.62 [†] [0.35, 0.79]	-0.07 [-0.21, 0.08]	0.68 [†] [0.41, 0.92]
bc	0.85 [†] [0.61, 0.95]	-0.08 [-0.27, 0.12]	0.92 [†] [0.68, 1.15]
Note: All confidence intervals are 95% BCa with 10,000 repetitions. † indicates that the CIs do not contain 0.			

353

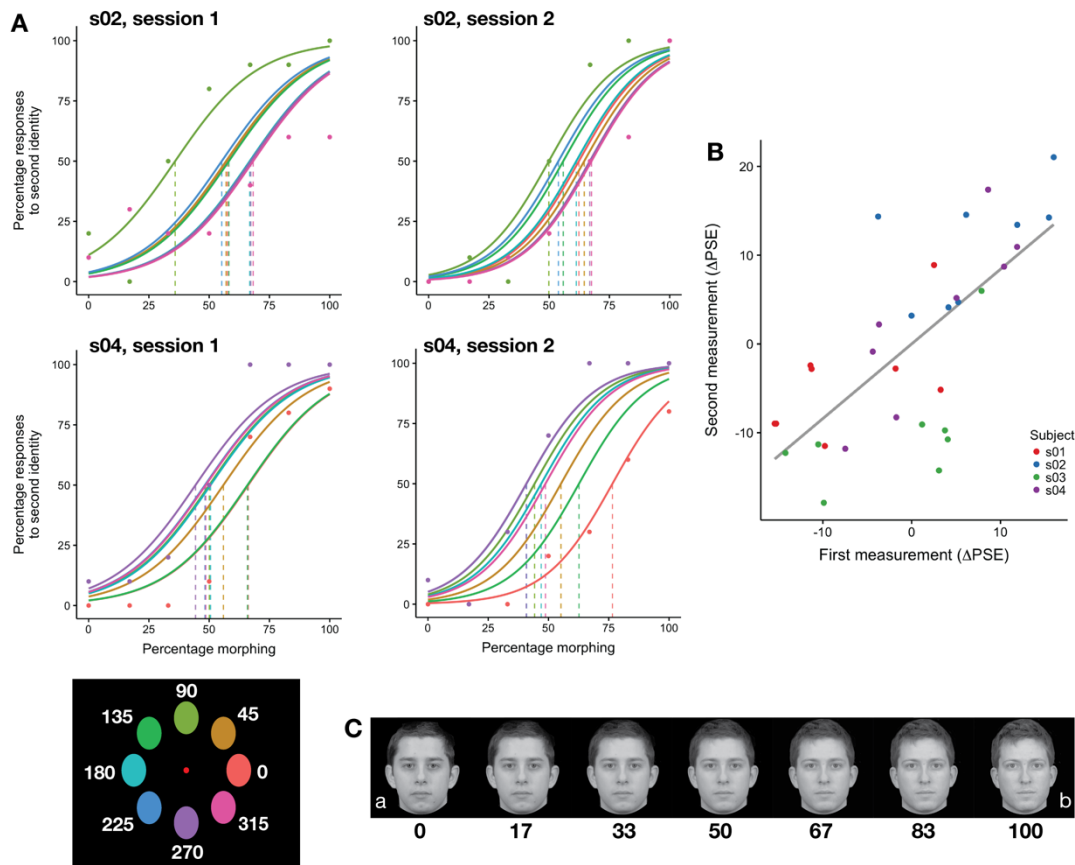


Figure 2. Stable and idiosyncratic biases in identification in Experiment 1. A) Psychometric fit for two subjects from both sessions. Colors indicate location (see colors in bottom left corner); actual data (points) are shown only for the extreme locations to avoid visual clutter. B) The parameter estimates across sessions (at least 33 days apart) were stable ($r = 0.71$ [0.47, 0.84], see Table 1). Dots represent

individual parameter estimates for each location, color coded according to each subject. Correlations were performed on the data shown in this panel. C) Example morphs used in the experiment. Note that the morphs depicted here are shown for illustration only, and participants saw morphs of identities that were personally familiar to them.

354

355

356 **Experiment 2**

357 In Experiment 1 participants exhibited stable, retinotopic biases for face identification
358 that were specific to each participant. Experiment 1, however, used only two target
359 identities, thus it could not address the question of whether the biases were specific to
360 target identities or to general variations in face recognition that would be the same
361 for all target faces. For this reason we conducted a second experiment in which we
362 increased the number of target identities. In Experiment 2, participants performed a
363 similar task as in Experiment 1 with the following differences. First, each face was
364 presented for 100 ms instead of 50 ms in order to make the task easier, since some
365 participants could not perform the task in Experiment 1; second, each face could
366 belong to one of three morphs, and participants were required to indicate which of
367 three identities the face belonged to; third, each face could appear in four retinal
368 locations instead of eight (see Figure 1) to maintain an appropriate duration of the
369 experiment. Each participant performed another experimental session at least 28
370 days after the first session (average 33 days \pm 8 days SD).

371 We found that participants exhibited stable biases across sessions for the three
372 morphs (see Table 1 and Figure 3). Interestingly, within-subjects correlations were
373 higher than between-subjects correlations for the two morphs that included the
374 identity *c* (morphs *ac* and *bc*), but not for morph *ab* (see Table 2), suggesting stronger
375 differences in spatial heterogeneity caused by identity *c*. To test this further, we
376 performed a two-way ANOVA on the PSE estimates across sessions with participants
377 and angular locations as factors. The ANOVA was run for each pair of morphs

378 containing the same identity (e.g., for identity *a* the ANOVA was run on data from
379 morphs *ab* and *ac*), and the PSE estimates were transformed to be with respect to the
380 same identity (e.g., for identity *b* we considered PSE_{bc} and $100 - PSE_{ab}$). We found
381 significant interactions between participants and angular locations for identity *b* ($F(27,$
382 $120) = 1.77, p = 0.01947$) and identity *c* ($F(27, 120) = 3.34, p = 3.229e-06$), but not
383 identity *a* ($F(27, 120) = 1.17, p = 0.2807$), confirming that participants showed increased
384 spatial heterogeneity for identities *b* and *c*. The increased spatial heterogeneity for
385 identities *b* and *c*, but not *a*, can be appreciated by inspecting the ΔPSE estimates for
386 each participant. Figure 4A shows lower bias across retinal locations for morph *ab*
387 than the other two morphs, suggesting more similar performance across locations for
388 morph *ab*. To investigate factors explaining the difference in performance across
389 spatial locations between the three identities, we compared the ΔPSE estimates with
390 the reported familiarity of the identities.

391 The variance of the average ΔPSE estimates across sessions for each subject was
392 significantly correlated with the reported familiarity of the identities
393 ($r = -0.56 [-0.71, -0.30], t(28) = -3.59, p = 0.001248$), showing that the strength of the
394 retinal bias for identities was inversely modulated by personal familiarity (see Figure
395 4B). We estimated personal familiarity by averaging participants' ratings of the
396 identities on three scales (Inclusion of the Other in the Self, the We-Scale, and the
397 Subjective Closeness Inventory, see Methods for details). The three scales were highly
398 correlated (min correlation $r = 0.89$, max correlation $r = 0.96$).

399 Because the amount of personal familiarity was correlated with the amount of contact
 400 with a target identity ($r = 0.45$ [0.17, 0.68], $t(28) = 2.65$,
 401 $p = 0.01304$), we tested whether a linear model predicting Δ PSE with both contact and
 402 familiarity as predictors could fit the data better. Both models were significant, but
 403 the model with two predictors provided a significantly better fit ($X^2(1) = 6.30$, $p =$
 404 0.0121 , log-likelihood ratio test), and explained more variance as indicated by higher
 405 R^2 : $R^2 = 0.45$, adjusted $R^2 = 0.40$ for the model with both Familiarity and Contact
 406 scores ($F(2, 27) = 10.82$, $p = 0.0003539$), and $R^2 = 0.32$, adjusted $R^2 = 0.29$ for the model
 407 with the Familiarity score only ($F(1, 28) = 12.88$, $p = 0.001248$). Importantly, both
 408 predictors were significant (see Table 3), indicating that familiarity modulated the
 409 variance of the Δ PSE estimates in addition to modulation based on the amount of
 410 contact with a person. After adjusting for the contact score, the variance of the Δ PSE
 411 estimates and the familiarity score were still significantly correlated ($r_p = -0.42$ [-0.61, -
 412 0.16], $t(28) = -2.42$, $p = 0.02235$).

Table 3. Models predicting variance of the Δ PSE estimates across locations in Experiment 2.

Model	R^2	Score	β	Δ_p^2	t	p
1	0.32	Familiarity	-0.0574	0.32	-3.59	0.0013
2	0.45	Familiarity	-0.0390	0.17	-2.38	0.0249
		Contact	-0.0452	0.19	-2.512	0.0183

413

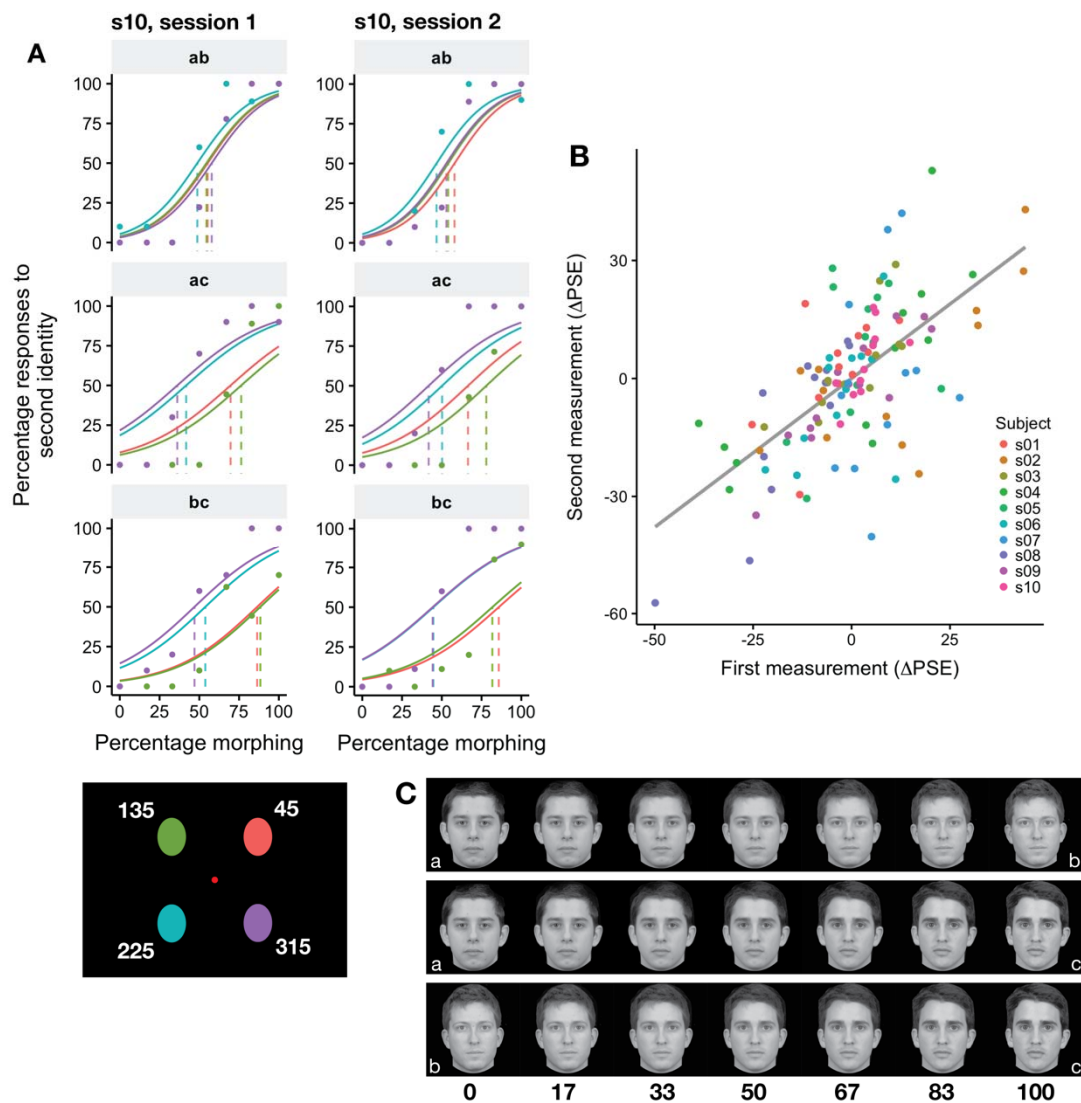


Figure 3. Stable and idiosyncratic biases in identification in Experiment 2. A) Psychometric fit for one subject from both sessions for each of the morphs. Colors indicate location (see colors in bottom left corner); actual data (points) are shown only for the extreme locations to avoid visual clutter. B) The parameter estimates across sessions (at least 28 days apart) were stable ($r = 0.64 [0.5, 0.75]$, see Table 1). Dots represent individual parameter estimates for each location, color coded according to each participant. Correlations were performed on the data shown in this panel. C) Example morphs used in the experiment. Note that the morphs depicted here are shown only for illustration (participants saw morphs of identities who were personally familiar).

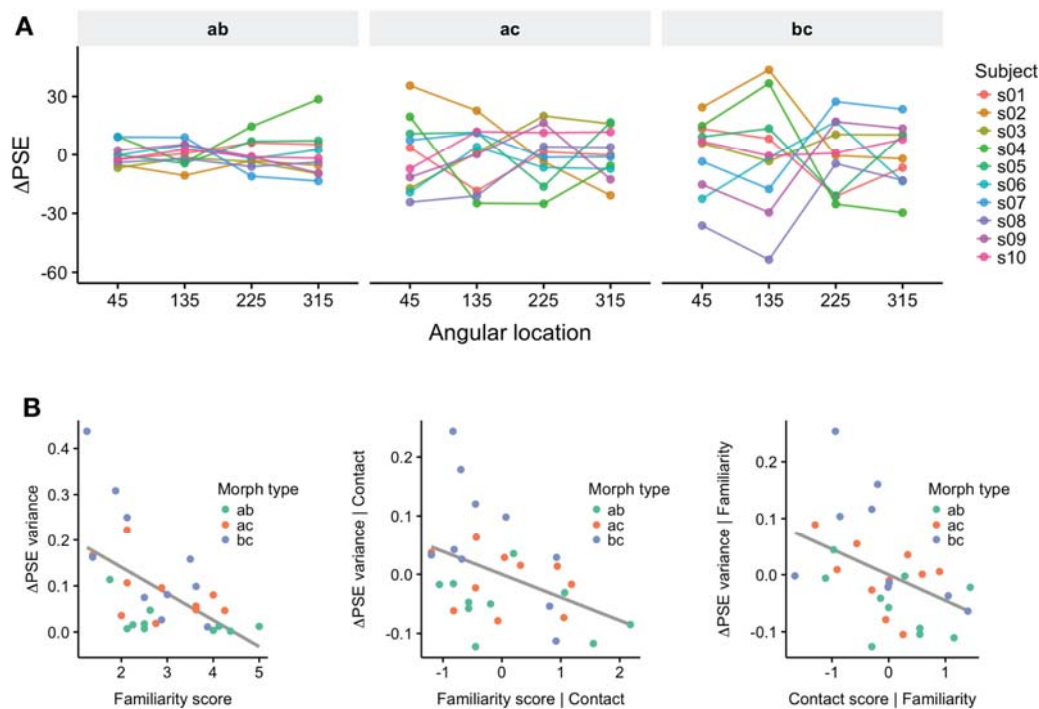


Figure 4. The strength of idiosyncratic biases was modulated by personal familiarity. A) Individual subjects' Δ PSE for each morph, averaged across sessions. Note the difference in variance across locations for the three different morphs (left to right)). B) The variance across locations of Δ PSE estimates was inversely correlated with the reported familiarity of the identities (left panel; $r = -0.56$ [-0.71, -0.30]), even when adjusting for the Contact score (middle panel; $r_p = -0.42$ [-0.61, -0.16]). The right panel shows the scatterplot between the Contact score and the Δ PSE variance, adjusted for the Familiarity score, which were significantly correlated as well ($r_p = -0.44$ [-0.62, -0.17]). See Methods for definition of the Familiarity score and the Contact score. Dots represent individual participant's data, color coded according to morph type. Correlations were performed on the data shown in these panels.

415

416

417 **Model simulation**

418 In two behavioral experiments we found a stable, idiosyncratic bias towards specific
419 identities that varied according to the location in which the morphed face stimuli
420 appeared. The bias was reduced with more familiar identities, showing effects of
421 learning. To account for this effect, we hypothesized that small populations of
422 neurons selective to specific identities sample a limited portion of the visual field
423 (Afraz et al., 2010). We also hypothesized that with extended interactions with a
424 person, more neural units become selective to the facial appearance of the identity. In
425 turn, this increases the spatial extent of the field covered by the population and thus
426 reduces the retinotopic bias.

427 To quantitatively test this hypothesis, we simulated a population of neural units in
428 IOG (OFA), pFus, and mFus using the Compressive Spatial Summation model (Kay et
429 al., 2013, 2015). The parameters of this model were estimated from published results
430 reported in Kay et al. (2015). We simulated learning effects by progressively increasing
431 the number of units selective to one of the two identities, and measuring the response
432 of a linear decoder trained to distinguish between the two identities. As can be seen in
433 Figure 5A, increasing the number of units reduced the overall bias (expressed as
434 variance against 0.5 of the PSE estimates, see *Methods* for details) by increasing the
435 spatial coverage (see Figure 5B). Interestingly, the larger bias was found within the
436 simulated IOG, because the stimuli shown at 7° of eccentricity were at the border of
437 the receptive field coverage (Figure 5B).

438 As an alternative explanation, we tested whether differences in gain could reduce the
 439 bias to a similar extent as increasing the number of units. Figure 5C shows that
 440 modulating the gain failed to reduce the retinotopic bias in all simulated ROIs.

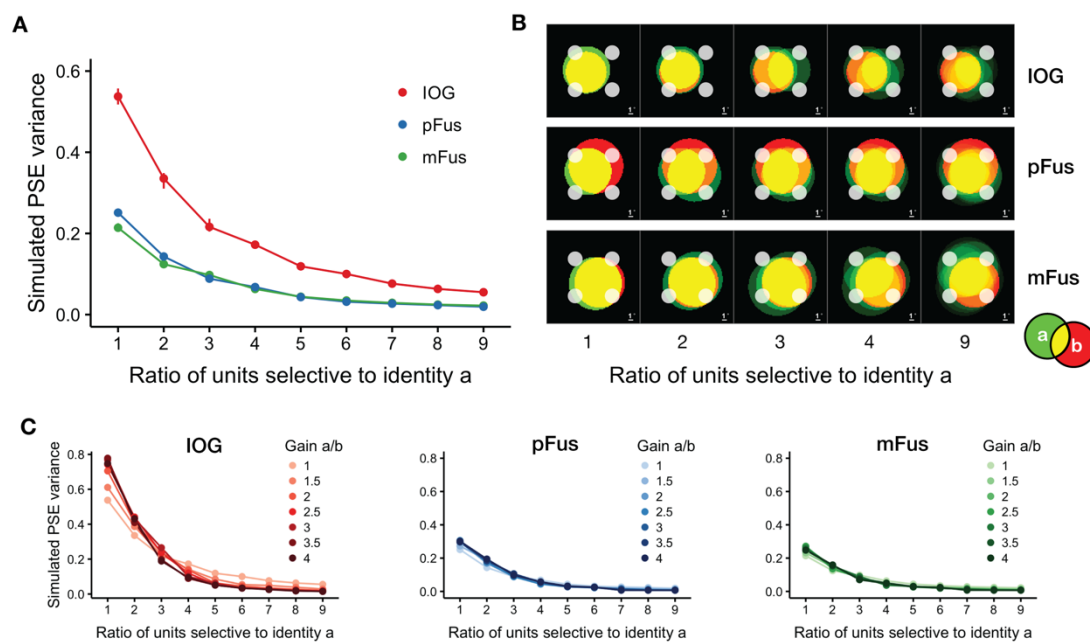


Figure 5. Simulating retinotopic biases and learning effects in face-responsive ROIs. We hypothesized that neural units (voxels, small populations of neurons, or individual neurons) cover a limited portion of the visual field, and that learning increases the number of neural units selective to a particular identity. A) Increasing the number of units selective to one identity reduces the retinotopic bias. Results of simulating 500 experiments by varying the ratio of neural units selective to one of two identities and fixing the gain to 1 for both identities. Dots represent median values with 68% bootstrapped CIs (1,000 replicates; note that for some points the CIs are too small to be seen). In all simulated ROIs the variance of the PSE around 50% decreases with increasing number of units selective to a, but remains larger in IOG because of its receptive field size. B) Example of increasing the number of units selective to one identity. Each colored circle represents the receptive field of a neural unit, color coded according to its preferential identity (green: identity *a*, red: identity *b*, yellow: overlap). Gray circles show location of the stimuli. Each column is normalized to the maximum number of units covering a portion of receptive field. Receptive field are shown as circles with radius 2σ , following the convention in Kay et al., (2015). In IOG, stimuli are at the border of the field covered by the simulated units, resulting in a larger bias across locations compared to pFus and mFus. C) Increasing the gain of the response to one identity fails to reduce the retinotopic bias. We repeated 500 simulated experiments as in A) and modulated the gain of the response of the units selective to identity *a*. Each dot represents median values

of PSE variance for 500 simulated experiments. CIs are not shown to reduce visual clutter.

441

442 **Discussion**

443 Afraz et al. (2010) reported spatial heterogeneity for recognition of facial attributes
444 such as gender and age, suggesting that relatively independent neural populations
445 tuned to facial features might sample different regions of the visual field. Prolonged
446 social interactions with personally familiar faces lead to facilitated, prioritized
447 processing of those faces. Here we wanted to investigate if this learning of face
448 identity through repeated social interactions also affects these local visual processes,
449 by measuring spatial heterogeneity of identity recognition. We measured whether
450 face identification performance for personally familiar faces differed according to the
451 location in the visual field where face images were presented. We found that
452 participants exhibited idiosyncratic, retinotopic biases for different face identities that
453 were stable across experimental sessions. Importantly, the variability of the
454 retinotopic bias was reduced with increased familiarity with the target identities.
455 These data support the hypothesis that familiarity modulates processes in visual areas
456 with limited position invariance (Visconti di Oleggio Castello et al., 2017a).

457 These results extend the reports of spatial heterogeneity in visual processing to face
458 identification. Similar biases exist for high-level judgments such as face gender and
459 age (Afraz et al., 2010), as well as shape discrimination (Afraz et al., 2010), crowding,
460 and saccadic precision (Greenwood et al., 2017). Afraz et al. (2010) suggested that

461 neurons in IT exhibit biases that are dependent on retinal location because their
462 receptive field sizes are not large enough to provide complete translational invariance,
463 and stimuli in different locations will activate a limited group of neurons. In this work,
464 we show that these perceptual biases for face processing not only exist for gender and
465 age judgments (Afraz et al., 2010), but also for face identification and that these
466 biases are affected by learning.

467 *Location-dependent coding in face-responsive areas*

468 Neurons in temporal cortex involved in object recognition are widely thought to be
469 invariant to object translation, that is their response to an object will not be
470 modulated by the location of the object in the visual field (Riesenhuber and Poggio,
471 1999; Hung et al., 2005). However, evidence suggests that location information is
472 preserved in activity of neurons throughout temporal cortex (Kravitz et al., 2008;
473 Hong et al., 2016). Location information can be encoded as a retinotopic map, such as
474 in early visual cortex, where neighboring neurons are selective to locations that are
475 neighboring in the visual field. In the absence of a clear cortical retinotopic map,
476 location information can still be preserved at the level of population responses
477 (Schwarzlose et al., 2008; Rajimehr et al., 2014; Henriksson et al., 2015; Kay et al.,
478 2015).

479 Areas of occipital and temporal cortices show responses to objects that are
480 modulated by position (Kravitz et al., 2008, 2010; Sayres and Grill-Spector, 2008). In
481 particular, also face-responsive areas of the ventral core system (Haxby et al., 2000;

482 Visconti di Oleggio Castello et al., 2017a) such as OFA, pFus, and mFus show
483 responses that are modulated by the position in which a face appears. Responses to a
484 face are stronger in these areas when faces are presented foveally rather than
485 peripherally (Levy et al., 2001; Hasson et al., 2002; Malach et al., 2002). In addition,
486 early face processing areas such as PL in monkeys or OFA in humans code specific
487 features of faces in typical locations. Neurons in PL are tuned to eyes in the
488 contralateral hemifield, with receptive fields covering the typical location of the eyes
489 at fixation (Issa and DiCarlo, 2012). Similarly, OFA responses to face parts are stronger
490 when they are presented in typical locations (de Haas et al., 2016), and OFA activity
491 codes the position and relationship between face parts (Henriksson et al., 2015).

492 The modulation of responses by object location in these areas seems to be driven by
493 differences in receptive field sizes. In humans, population receptive fields (pRF) can be
494 estimated with fMRI by modeling voxel-wise BOLD responses (Dumoulin and
495 Wandell, 2008; Wandell and Winawer, 2011, 2015; Kay et al., 2013). These studies
496 have shown that pRF centers are mostly located in the contralateral hemifield (Kay et
497 al., 2015; Grill-Spector et al., 2017b), corresponding to the reported preference of
498 these areas for faces presented contralaterally (Hemond et al., 2007). In addition, pRF
499 sizes increase the higher in the face processing hierarchy, favoring perifoveal regions
500 (Kay et al., 2015; Silson et al., 2016). The location-dependent coding of faces in these
501 face-processing areas might be based on population activity, since these areas do not
502 overlap with retinotopic maps in humans (for example, OFA does not seem to overlap
503 with estimated retinotopic maps, Silson et al., 2016, but see Janssens et al., 2014;

504 Rajimehr et al., 2014; Arcaro and Livingstone, 2017; Arcaro et al., 2017 for work in
505 monkeys showing partial overlap between retinotopic maps and face patches).

506 *Cortical origin of idiosyncratic biases and effects of familiarity*

507 Populations of neurons in visual areas and in temporal cortex cover limited portions of
508 the visual field, with progressively larger receptive fields centered around perifoveal
509 regions (Grill-Spector et al., 2017b). This property suggests that biases in high-level
510 judgments of gender, age, and identity may be due to the variability of feature
511 detectors that cover limited portions of the visual field (Afraz et al., 2010). While the
512 results from our behavioral study cannot point to a precise location of the cortical
513 origin of these biases, our computational simulation suggests that a larger bias could
514 arise from responses in the OFA, given the estimates of receptive field size and
515 eccentricity in this area (Kay et al., 2015; Grill-Spector et al., 2017b). We cannot
516 exclude that this bias might originate in earlier areas of the visual processing stream.

517 In this work, we showed that the extent of variation in biases across retinal locations
518 was inversely correlated with the reported familiarity with individuals, suggesting that
519 a history of repeated interaction with a person may tune the responses of neurons to
520 that individual in different retinal locations, generating more homogeneous
521 responses. Repeated exposure to the faces of familiar individuals during real-life social
522 interactions results in a detailed representation of the visual appearance of a
523 personally familiar face. Our computational simulation suggests a simple process for
524 augmenting and strengthening the representation of a face. Learning through social

525 interactions might cause a greater number of neural units to become responsive to a
526 specific identity, thus covering a larger area of the visual field and reducing the
527 retinotopic biases. Our results showed that both ratings of familiarity and ratings of
528 amount of contact were strong predictors for reduced retinotopic bias; however,
529 familiarity still predicted the reduced bias when accounting for amount of contact.
530 While additional experiments are needed to test whether pure perceptual learning is
531 sufficient to reduce the retinotopic biases to the same extent as personal familiarity,
532 these results suggest that repeated personal interactions can strengthen neural
533 representations to a larger extent than mere increased frequency of exposure to a
534 face. This idea is consistent with neuroimaging studies showing a stronger and more
535 widespread activation for personally familiar faces compared to unfamiliar or
536 experimentally learned faces (Gobbini and Haxby, 2006; Cloutier et al., 2011; Natu and
537 O'Toole, 2011; Leibenluft et al., 2004; Gobbini and Haxby, 2007; Bobes et al., 2013;
538 Ramon and Gobbini, 2017; Visconti di Oleggio Castello et al., 2017a).

539 *Effects of attention*

540 Could differences in attention explain the modulation of retinotopic biases reported
541 here? Faces, and personally familiar faces in particular, are important social stimuli
542 whose correct detection and processing affects social behavior (Brothers, 2002;
543 Gobbini and Haxby, 2007). Behavioral experiments from our lab have shown that
544 personally familiar faces break through faster in a continuous flash suppression
545 paradigm (Gobbini et al., 2013), and hold attention more strongly than unfamiliar
546 faces do in a Posner cueing paradigm (Chauhan et al., 2017). These results show that

547 familiar faces differ not only at the level of representations, but also in allocation of
548 attention. At the neural level, changes in attention might be implemented as
549 increased gain for salient stimuli or increased receptive field size (Kay et al., 2015). In
550 an fMRI experiment Kay et al. (2015) reported that population receptive field (pRF)
551 estimates were modulated by the type of task. Gain, eccentricity, and size of the pRFs
552 increased during a 1-back repetition detection task on facial identity as compared to a
553 1-back task on digits presented foveally.

554 To address differences in gain in our computational simulation, we modified the
555 relative gain of units responsive to one of the two identities and found that it did not
556 influence the PSE bias across locations. This bias was more strongly modulated by the
557 number of units responsive to one of the identities. On the other hand, increases in
558 receptive field size and eccentricity could reduce the bias, as shown by differences
559 between the simulated ROIs. However, while the bias was reduced in pFus compared
560 to IOG, for example, the difference in receptive field size (3.68° vs 2.75°) was not
561 sufficient to eliminate the bias with a limited number of neural units. While this result
562 cannot rule out attentional effects completely, it suggests that the retinotopic biases
563 for identification are more strongly modulated by the uneven coverage of the visual
564 field by a limited number of neural units. Additional experiments are needed to
565 further characterize the differences in attention and representations that contribute
566 to the facilitated processing of personally familiar faces.

567 *Implications for computational models of vision*

568 Many computational models of biological vision posit translational invariance:
569 neurons in IT are assumed to respond to the same extent, regardless of the object
570 position (Riesenhuber and Poggio, 1999; Serre et al., 2007; Kravitz et al., 2008). Even
571 the models that currently provide better fits to neural activity in IT such as
572 hierarchical, convolutional neural networks (Yamins et al., 2014; Kriegeskorte, 2015;
573 Yamins and DiCarlo, 2016) use weight sharing in convolutional layers to achieve
574 position invariance (LeCun et al., 2015; Schmidhuber, 2015; Goodfellow et al., 2016).
575 While this reduces complexity by limiting the number of parameters to be fitted,
576 neuroimaging and behavioral experiments have shown that translational invariance in
577 IT is preserved only for small displacements (DiCarlo and Maunsell, 2003; Kay et al.,
578 2015; Silson et al., 2016; for a review see Kravitz et al., 2008), with varying receptive
579 field sizes and eccentricities (Grill-Spector et al., 2017a). Our results highlight the
580 limited position invariance for high-level judgments such as identity, and add to the
581 known spatial heterogeneity for gender and age judgments (Afraz et al., 2010). Our
582 results also show that a higher degree of invariance can be achieved through learning,
583 as shown by the reduced bias for highly familiar faces. This finding highlights that to
584 increase biological plausibility of models of vision, differences in eccentricity and
585 receptive field size should be taken into account (Poggio et al., 2014), as well as more
586 dynamic effects such as changes induced by learning and attention (Grill-Spector et
587 al., 2017a).

588 *Conclusions*

589 Taken together, the results reported here support our hypothesis that facilitated
590 processing for personally familiar faces might be mediated by the development or
591 tuning of detectors for personally familiar faces in the visual pathway in areas that still
592 have localized analyses (Gobbini et al., 2013; Visconti di Oleggio Castello et al., 2014,
593 2017b; Visconti di Oleggio Castello and Ida Gobbini, 2015). The OFA might be a
594 candidate for the cortical origin of these biases as well as for the development of
595 detectors for diagnostic fragments. Patterns of responses in OFA (and neurons in the
596 monkey putative homologue PL, Issa and DiCarlo, 2012) are tuned to typical locations
597 of face fragments (Henriksson et al., 2015; de Haas et al., 2016). Population receptive
598 fields of voxels in this region cover an area of the visual field that is large enough to
599 integrate features of intermediate complexity at an average conversational distance
600 (Kay et al., 2015; Grill-Spector et al., 2017b), such as combinations of eyes and
601 eyebrows, which have been shown to be theoretically optimal and highly informative
602 for object classification (Ullman et al., 2001, 2002; Ullman, 2007).

603 Future research is needed to further disambiguate differences in representations or
604 attention that generate these biases and how learning reduces them. Nonetheless,
605 our results suggest that prioritized processing for personally familiar faces may exist
606 at relatively early stages of the face processing hierarchy, as shown by the local biases
607 reported here. Learning associated with repeated personal interactions modifies the
608 representation of these faces, suggesting that personal familiarity affects face-
609 processing areas well after developmental critical periods (Arcaro et al., 2017;
610 Livingstone et al., 2017). We hypothesize that these differences may be one of the

611 mechanisms that underlies the known behavioral advantages for perception of
612 personally familiar faces (Burton et al., 1999; Gobbini and Haxby, 2007; Gobbini, 2010;
613 Gobbini et al., 2013; Visconti di Oleggio Castello et al., 2014, 2017b; Ramon et al.,
614 2015; Visconti di Oleggio Castello and Gobbini, 2015; Chauhan et al., 2017; Ramon and
615 Gobbini, 2017).

616

617 **References**

- 618 Afraz A, Pashkam MV, Cavanagh P (2010) Spatial heterogeneity in the perception of
619 face and form attributes. *Curr Biol* 20:2112–2116.
- 620 Arcaro MJ, Livingstone MS (2017) A hierarchical, retinotopic proto-organization of the
621 primate visual system at birth. *Elife* 6
- 622 Arcaro MJ, Schade PF, Vincent JL, Ponce CR, Livingstone MS (2017) Seeing faces is
623 necessary for face-domain formation. *Nat Neurosci*
- 624 Aron A, Aron EN, Smollan D (1992) Inclusion of Other in the Self Scale and the
625 structure of interpersonal closeness. *J Pers Soc Psychol* 63:596.
- 626 Barragan-Jason G, Cauchoix M, Barbeau EJ (2015) The neural speed of familiar face
627 recognition. *Neuropsychologia* 75:390–401.
- 628 Bates D, Mächler M, Bolker B, Walker S (2015) Fitting Linear Mixed-Effects Models
629 Using lme4. *J Stat Softw* 67:1–48.
- 630 Berscheid E, Snyder M, Omoto AM (1989) The Relationship Closeness Inventory:
631 Assessing the closeness of interpersonal relationships. *J Pers Soc Psychol*
632 57:792.
- 633 Bobes MA, Lage Castellanos A, Quiñones I, García L, Valdes-Sosa M (2013) Timing and
634 tuning for familiarity of cortical responses to faces. *PLoS One* 8:e76100.
- 635 Brothers L (2002) The social brain: a project for integrating primate behavior and
636 neurophysiology in a new domain. *Foundations in social neuroscience*:367–385.
- 637 Bruce V, Young A (1986) Understanding face recognition. *Br J Psychol* 77 (Pt 3):305–
638 327.
- 639 Burton AM, Wilson S, Cowan M, Bruce V (1999) Face Recognition in Poor-Quality
640 Video: Evidence From Security Surveillance. *Psychol Sci* 10:243–248.
- 641 Chauhan V, Visconti di Oleggio Castello M, Soltani A, Gobbin MI (2017) Social
642 Saliency of the Cue Slows Attention Shifts. *Front Psychol* 8:738.
- 643 Cialdini RB, Brown SL, Lewis BP, Luce C, Neuberg SL (1997) Reinterpreting the
644 empathy--altruism relationship: When one into one equals oneness. *J Pers Soc*
645 *Psychol* 73:481.

- 646 Cloutier J, Kelley WM, Heatherton TF (2011) The influence of perceptual and
647 knowledge-based familiarity on the neural substrates of face perception. *Soc*
648 *Neurosci* 6:63–75.
- 649 Cortes C, Vapnik V (1995) Support-vector networks. *Mach Learn* 20:273–297.
- 650 de Haas B, Schwarzkopf DS, Alvarez I, Lawson RP, Henriksson L, Kriegeskorte N, Rees
651 G (2016) Perception and Processing of Faces in the Human Brain Is Tuned to
652 Typical Feature Locations. *J Neurosci* 36:9289–9302.
- 653 Diamond R, Carey S (1986) Why faces are and are not special: An effect of expertise. *J*
654 *Exp Psychol Gen* 115:107.
- 655 DiCarlo JJ, Maunsell JHR (2003) Anterior inferotemporal neurons of monkeys engaged
656 in object recognition can be highly sensitive to object retinal position. *J*
657 *Neurophysiol* 89:3264–3278.
- 658 Dumoulin SO, Wandell BA (2008) Population receptive field estimates in human visual
659 cortex. *Neuroimage* 39:647–660.
- 660 Efron B (1987) Better Bootstrap Confidence Intervals. *J Am Stat Assoc* 82:171–185.
- 661 Faul F, Erdfelder E, Buchner A, Lang A-G (2009) Statistical power analyses using
662 G*Power 3.1: tests for correlation and regression analyses. *Behav Res Methods*
663 41:1149–1160.
- 664 Faul F, Erdfelder E, Lang A-G, Buchner A (2007) G*Power 3: a flexible statistical power
665 analysis program for the social, behavioral, and biomedical sciences. *Behav Res*
666 *Methods* 39:175–191.
- 667 Gächter S, Starmer C, Tufano F (2015) Measuring the Closeness of Relationships: A
668 Comprehensive Evaluation of the “Inclusion of the Other in the Self” Scale.
669 *PLoS One* 10:e0129478.
- 670 Gobbini MI (2010) Distributed process for retrieval of person knowledge. *Social*
671 *neuroscience: Toward understanding the underpinnings of the social mind*:40–
672 53.
- 673 Gobbini MI, Gors JD, Halchenko YO, Rogers C, Guntupalli JS, Hughes H, Cipolli C
674 (2013) Prioritized Detection of Personally Familiar Faces. *PLoS One* 8:e66620.
- 675 Gobbini MI, Haxby JV (2006) Neural response to the visual familiarity of faces. *Brain*
676 *Res Bull* 71:76–82.

- 677 Gobbini MI, Haxby JV (2007) Neural systems for recognition of familiar faces.
678 *Neuropsychologia* 45:32–41.
- 679 Goodfellow I, Bengio Y, Courville A, Bengio Y (2016) Deep learning. MIT press
680 Cambridge.
- 681 Greenwood JA, Szinte M, Sayim B, Cavanagh P (2017) Variations in crowding, saccadic
682 precision, and spatial localization reveal the shared topology of spatial vision.
683 *Proc Natl Acad Sci U S A* 114:E3573–E3582.
- 684 Grill-Spector K, Kay K, Weiner KS (2017a) The Functional Neuroanatomy of Face
685 Processing: Insights from Neuroimaging and Implications for Deep Learning. In:
686 Deep Learning for Biometrics (Bhanu B, Kumar A, eds), pp 3–31 *Advances in*
687 *Computer Vision and Pattern Recognition*. Cham: Springer International
688 Publishing.
- 689 Grill-Spector K, Weiner KS, Kay K, Gomez J (2017b) The Functional Neuroanatomy of
690 Human Face Perception. *Annu Rev Vis Sci* 3:167–196.
- 691 Guntupalli JS, Gobbini MI (2017) Reading Faces: From Features to Recognition. *Trends*
692 *Cogn Sci* 21:915–916.
- 693 Hasson U, Levy I, Behrmann M, Hendler T, Malach R (2002) Eccentricity bias as an
694 organizing principle for human high-order object areas. *Neuron* 34:479–490.
- 695 Haxby JV, Hoffman EA, Gobbini MI (2000) The distributed human neural system for
696 face perception. *Trends Cogn Sci* 4:223–233.
- 697 Hemond CC, Kanwisher NG, Op de Beeck HP (2007) A Preference for Contralateral
698 Stimuli in Human Object- and Face-Selective Cortex. *PLoS One* 2:e574.
- 699 Henriksson L, Mur M, Kriegeskorte N (2015) Faciotopy-A face-feature map with face-
700 like topology in the human occipital face area. *Cortex* 72:156–167.
- 701 Hong H, Yamins DLK, Majaj NJ, DiCarlo JJ (2016) Explicit information for category-
702 orthogonal object properties increases along the ventral stream. *Nat Neurosci*
703 19:613–622.
- 704 Hung CP, Kreiman G, Poggio T, DiCarlo JJ (2005) Fast readout of object identity from
705 macaque inferior temporal cortex. *Science* 310:863–866.
- 706 Idson LC, Mischel W (2001) The personality of familiar and significant people: the lay
707 perceiver as a social-cognitive theorist. *J Pers Soc Psychol* 80:585–596.

- 708 Issa EB, DiCarlo JJ (2012) Precedence of the Eye Region in Neural Processing of Faces.
709 Journal of Neuroscience 32:16666–16682.
- 710 Janssens T, Zhu Q, Popivanov ID, Vanduffel W (2014) Probabilistic and single-subject
711 retinotopic maps reveal the topographic organization of face patches in the
712 macaque cortex. J Neurosci 34:10156–10167.
- 713 Kay KN, Weiner KS, Grill-Spector K (2015) Attention reduces spatial uncertainty in
714 human ventral temporal cortex. Curr Biol 25:595–600.
- 715 Kay KN, Winawer J, Mezer A, Wandell BA (2013) Compressive spatial summation in
716 human visual cortex. J Neurophysiol 110:481–494.
- 717 Kleiner M, Brainard D, Pelli D, Ingling A, Murray R (2007) What’s new in Psychtoolbox-
718 3. Perception
- 719 Kravitz DJ, Kriegeskorte N, Baker CI (2010) High-level visual object representations
720 are constrained by position. Cereb Cortex 20:2916–2925.
- 721 Kravitz DJ, Vinson LD, Baker CI (2008) How position dependent is visual object
722 recognition? Trends Cogn Sci 12:114–122.
- 723 Kriegeskorte N (2015) Deep Neural Networks: A New Framework for Modeling
724 Biological Vision and Brain Information Processing. Annual Review of Vision
725 Science 1:417–446.
- 726 LeCun Y, Bengio Y, Hinton G (2015) Deep learning. Nature 521:436–444.
- 727 Leibenluft E, Gobbin MI, Harrison T, Haxby JV (2004) Mothers’ neural activation in
728 response to pictures of their children and other children. Biol Psychiatry
729 56:225–232.
- 730 Levy I, Hasson U, Avidan G, Hendler T, Malach R (2001) Center–periphery
731 organization of human object areas. Nat Neurosci 4:533–539.
- 732 Livingstone MS, Vincent JL, Arcaro MJ, Srihasam K, Schade PF, Savage T (2017)
733 Development of the macaque face-patch system. Nat Commun 8:14897.
- 734 Malach R, Levy I, Hasson U (2002) The topography of high-order human object areas.
735 Trends Cogn Sci 6:176–184.
- 736 Moscatelli A, Mezzetti M, Lacquaniti F (2012) Modeling psychophysical data at the
737 population-level: the generalized linear mixed model. J Vis 12

- 738 Naselaris T, Kay KN, Nishimoto S, Gallant JL (2011) Encoding and decoding in fMRI.
739 Neuroimage 56:400–410.
- 740 Natu V, O’Toole AJ (2011) The neural processing of familiar and unfamiliar faces: A
741 review and synopsis. Br J Psychol 102:726–747.
- 742 Poggio T, Mutch J, Isik L (2014) Computational role of eccentricity dependent cortical
743 magnification. arXiv [csLG]
- 744 Rajimehr R, Bilenko NY, Vanduffel W, Tootell RBH (2014) Retinotopy versus Face
745 Selectivity in Macaque Visual Cortex. J Cogn Neurosci 22:1–10.
- 746 Ramon M, Gobbini MI (2017) Familiarity matters: A review on prioritized processing of
747 personally familiar faces. Vis cogn:1–17.
- 748 Ramon M, Vizioli L, Liu-Shuang J, Rossion B (2015) Neural microgenesis of personally
749 familiar face recognition. Proc Natl Acad Sci U S A 112:E4835–E4844.
- 750 Riesenhuber M, Poggio T (1999) Hierarchical models of object recognition in cortex.
751 Nat Neurosci 2:1019–1025.
- 752 Sayres R, Grill-Spector K (2008) Relating retinotopic and object-selective responses in
753 human lateral occipital cortex. J Neurophysiol 100:249–267.
- 754 Schmidhuber J (2015) Deep learning in neural networks: An overview. Neural Netw
755 61:85–117.
- 756 Schwarzlose RF, Swisher JD, Dang S, Kanwisher N (2008) The distribution of category
757 and location information across object-selective regions in human visual cortex.
758 Proc Natl Acad Sci U S A 105:4447–4452.
- 759 Serre T, Oliva A, Poggio T (2007) A Feedforward Architecture Accounts for Rapid
760 Categorization. Proc Natl Acad Sci U S A 104:6424–6429.
- 761 Silson EH, Groen IIA, Kravitz DJ, Baker CI (2016) Evaluating the correspondence
762 between face-, scene-, and object-selectivity and retinotopic organization
763 within lateral occipitotemporal cortex. J Vis 16:14.
- 764 Sugiura M (2014) Neuroimaging studies on recognition of personally familiar people.
765 Front Biosci 19:672–686.

- 766 Taylor MJ, Arsalidou M, Bayless SJ, Morris D, Evans JW, Barbeau EJ (2009) Neural
767 correlates of personally familiar faces: parents, partner and own faces. *Hum*
768 *Brain Mapp* 30:2008–2020.
- 769 Ullman S (2007) Object recognition and segmentation by a fragment-based hierarchy.
770 *Trends Cogn Sci* 11:58–64.
- 771 Ullman S, Sali E, Vidal-Naquet M (2001) A Fragment-Based Approach to Object
772 Representation and Classification. In: *Visual Form 2001*, pp 85–100. Springer,
773 Berlin, Heidelberg.
- 774 Ullman S, Vidal-Naquet M, Sali E (2002) Visual features of intermediate complexity
775 and their use in classification. *Nat Neurosci*
- 776 Visconti di Oleggio Castello M, Guntupalli JS, Yang H, Gobbini MI (2014) Facilitated
777 detection of social cues conveyed by familiar faces. *Front Hum Neurosci* 8:678.
- 778 Visconti di Oleggio Castello M, Halchenko YO, Guntupalli JS, Gors JD, Gobbini MI
779 (2017a) The neural representation of personally familiar and unfamiliar faces in
780 the distributed system for face perception. *Sci Rep* 7:12237.
- 781 Visconti di Oleggio Castello M, Ida Gobbini M (2015) Familiar Face Detection in 180ms.
782 *PLoS One* 10:e0136548.
- 783 Visconti di Oleggio Castello M, Wheeler KG, Cipolli C, Gobbini MI (2017b) Familiarity
784 facilitates feature-based face processing. *PLoS One* 12:e0178895.
- 785 Wandell BA, Winawer J (2011) Imaging retinotopic maps in the human brain. *Vision*
786 *Res* 51:718–737.
- 787 Wandell BA, Winawer J (2015) Computational neuroimaging and population receptive
788 fields. *Trends Cogn Sci* 19:349–357.
- 789 Willenbockel V, Sadr J, Fiset D, Horne GO, Gosselin F, Tanaka JW (2010) Controlling
790 low-level image properties: The SHINE toolbox. *Behav Res Methods* 42:671–
791 684.
- 792 Yamins DLK, DiCarlo JJ (2016) Using goal-driven deep learning models to understand
793 sensory cortex. *Nat Neurosci* 19:356–365.
- 794 Yamins DLK, Hong H, Cadieu CF, Solomon EA, Seibert D, DiCarlo JJ (2014)
795 Performance-optimized hierarchical models predict neural responses in higher
796 visual cortex. *Proc Natl Acad Sci U S A* 111:8619–8624.

797 Young AW, Burton AM (2017) Are We Face Experts? Trends Cogn Sci

798

799 Legends

800 **Figure 1. Experimental paradigm.** The left panel shows the experimental paradigm,
801 while the right panel shows the locations used in Experiment 1 (eight locations, top
802 panel) and in Experiment 2 (four locations, bottom panel).

803 **Figure 2. Stable and idiosyncratic biases in identification in Experiment 1.** A)
804 Psychometric fit for two subjects from both sessions. Colors indicate location (see
805 colors in bottom left corner); actual data (points) are shown only for the extreme
806 locations to avoid visual clutter. B) The parameter estimates across sessions (at least
807 33 days apart) were stable ($r = 0.71 [0.47, 0.84]$, see Table 1). Dots represent individual
808 parameter estimates for each location, color coded according to each subject.
809 Correlations were performed on the data shown in this panel. C) Example morphs
810 used in the experiment. Note that the morphs depicted here are shown for illustration
811 only, and participants saw morphs of identities that were personally familiar to them.

812 **Figure 3. Stable and idiosyncratic biases in identification in Experiment 2.** A)
813 Psychometric fit for one subject from both sessions for each of the morphs. Colors
814 indicate location (see colors in bottom left corner); actual data (points) are shown only
815 for the extreme locations to avoid visual clutter. B) The parameter estimates across
816 sessions (at least 28 days apart) were stable ($r = 0.64 [0.5, 0.75]$, see Table 1). Dots
817 represent individual parameter estimates for each location, color coded according to
818 each participant. Correlations were performed on the data shown in this panel. C)
819 Example morphs used in the experiment. Note that the morphs depicted here are
820 shown only for illustration (participants saw morphs of identities who were personally
821 familiar).

822 **Figure 4. The strength of idiosyncratic biases was modulated by personal**
823 **familiarity.** A) Individual subjects' Δ PSE for each morph, averaged across sessions.
824 Note the difference in variance across locations for the three different morphs (left to
825 right)). B) The variance across locations of Δ PSE estimates was inversely correlated
826 with the reported familiarity of the identities (left panel; $r = -0.56 [-0.71, -0.30]$), even
827 when adjusting for the Contact score (middle panel; $r_p = -0.42 [-0.61, -0.16]$). The right
828 panel shows the scatterplot between the Contact score and the Δ PSE variance,
829 adjusted for the Familiarity score, which were significantly correlated as well ($r_p = -$
830 $0.44 [-0.62, -0.17]$). See Methods for definition of the Familiarity score and the
831 Contact score. Dots represent individual participant's data, color coded according to
832 morph type. Correlations were performed on the data shown in these panels.

833 **Figure 5. Simulating retinotopic biases and learning effects in face-responsive**
834 **ROIs.** We hypothesized that neural units (voxels, small populations of neurons, or
835 individual neurons) cover a limited portion of the visual field, and that learning
836 increases the number of neural units selective to a particular identity. A) Increasing
837 the number of units selective to one identity reduces the retinotopic bias. Results of
838 simulating 500 experiments by varying the ratio of neural units selective to one of two

839 identities and fixing the gain to 1 for both identities. Dots represent median values
840 with 68% bootstrapped CIs (1,000 replicates; note that for some points the CIs are too
841 small to be seen). In all simulated ROIs the variance of the PSE around 50% decreases
842 with increasing number of units selective to a , but remains larger in IOG because of its
843 receptive field size. B) Example of increasing the number of units selective to one
844 identity. Each colored circle represents the receptive field of a neural unit, color coded
845 according to its preferential identity (green: identity a , red: identity b , yellow:
846 overlap). Gray circles show location of the stimuli. Each column is normalized to the
847 maximum number of units covering a portion of receptive field. Receptive field are
848 shown as circles with radius 2σ , following the convention in Kay et al., (2015). In IOG,
849 stimuli are at the border of the field covered by the simulated units, resulting in a
850 larger bias across locations compared to pFus and mFus. C) Increasing the gain of the
851 response to one identity fails to reduce the retinotopic bias. We repeated 500
852 simulated experiments as in A) and modulated the gain of the response of the units
853 selective to identity a . Each dot represents median values of PSE variance for 500
854 simulated experiments. CIs are not shown to reduce visual clutter.

855 **Table 1.** Correlation of parameter estimates across sessions for the two experiments.

856 **Table 2.** Comparison of within-subjects correlations of parameter estimates across
857 sessions with between-subjects correlations.

858 **Table 3.** Models predicting variance of the Δ PSE estimates across angular locations in
859 Experiment 2.

860 **Extended Data.** The archive contains data from both experiments, as well as the
861 analysis scripts.

862

863 **Tables**

Table 1. Correlation of parameter estimates across sessions for the two experiments.			
Parameter	r	t	df
Experiment 1			
PSE	0.89 [-0.23, 1]	4.86**	6
ΔPSE	0.71 [0.47, 0.84]	5.47***	30
Experiment 2			
PSE	0.98 [0.93, 0.99]	15.22***	10
ΔPSE	0.64 [0.5, 0.75]	9.02***	118
Note: All confidence intervals are 95% BCa with 10,000 repetitions. * $p < .05$. ** $p < .01$. *** $p < .001$			

864

Table 2. Comparison of within-subjects correlations of parameter estimates across sessions with between-subjects correlations.			
Morph	Within-subjects r	Between-subjects r	Difference
Experiment 1			
ab	0.65 [†] [0.57, 0.8]	-0.22 [-0.41, -0.01]	0.87 [†] [0.63, 1.1]
Experiment 2			
ab	0.32 [-0.10, 0.62]	-0.02 [-0.15, 0.11]	0.34 [-0.07, 0.69]
ac	0.62 [†] [0.35, 0.79]	-0.07 [-0.21, 0.08]	0.68 [†] [0.41, 0.92]
bc	0.85 [†] [0.61, 0.95]	-0.08 [-0.27, 0.12]	0.92 [†] [0.68, 1.15]
Note: All confidence intervals are 95% BCa with 10,000 repetitions. [†] indicates that the CIs do not contain 0.			

865

Table 3. Models predicting variance of the Δ PSE estimates across angular locations in Experiment 2.

Model	R ²	Score	β	σ_p^2	t	p
1	0.32	Familiarity	-0.0574	0.32	-3.59	0.0013
2	0.45	Familiarity	-0.0390	0.17	-2.38	0.0249
		Contact	-0.0452	0.19	-2.512	0.0183

866